nature nanotechnology

SUPPLEMENTARY INFORMATION

DOI: 10.1038/NNANO.2012.35

Stable Cycling of Double-Walled Silicon Nanotube Battery Anodes through Solid-Electrolyte Interphase Control

Hui Wu,[1*] Gerentt Chan,[2*] Jang Wook Choi,[1,3] Ill Ryu,[1] Yan Yao,[1] Matthew T. McDowell,[1] Seok Woo Lee,[1] Ariel Jackson,[1] Yuan Yang,[1] Liangbing Hu[1] and Yi Cui[1,□]

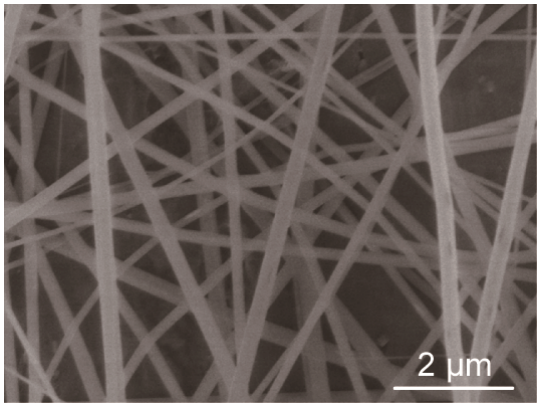

Figure S1. Scanning electron microscope (SEM) image of electrospun carbon nanofibers.

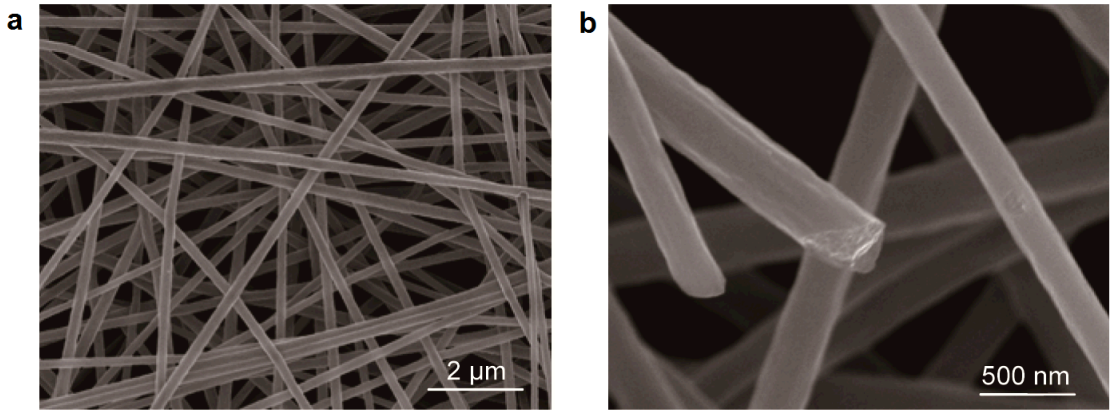

Figure S2. SEM images of silicon coated carbon nanofibers with low (a) and high (b) magnification.

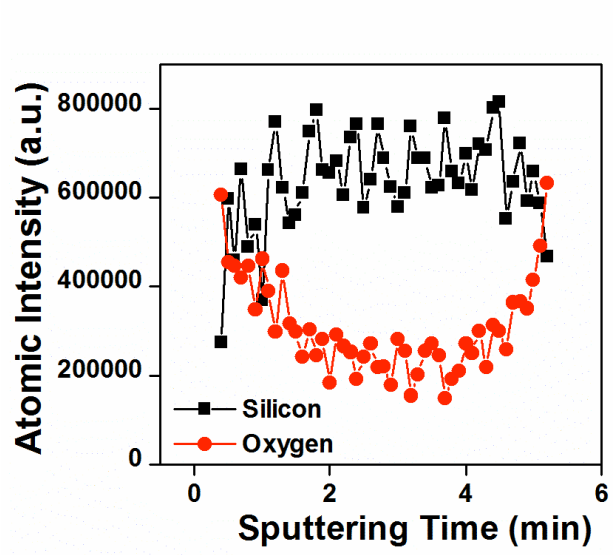

Figure S3. Auger depth profiling of DWSiNTs, showing double layer tube structure with oxide shell on the outside. During the initial sputtering both Si and O are present, corresponding to the outer SiOx wall of the nanotubes. Working through the inner silicon wall from t=1-3min, little O intensity is observed. From t=4-5min, the sputtering has bored through the first Si wall and has started on the Si wall on the other side, working outwards. The thickness of the outer SiOx wall was determined to be ~10 nm and the inner Si wall is ~20 nm, which is consistent with the transmission electron microscope (TEM) study (Fig. S4). The results of the Auger electron spectroscopy depth profiling clearly show that our proposed DWSiNTs are successfully synthesized.

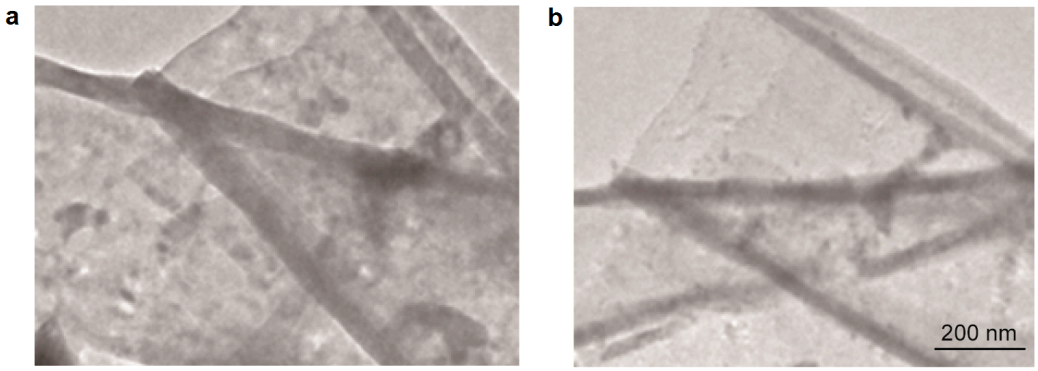

Figure S4. TEM images of an individual DWSiNT before (a) and after (b) remove surface oxide layer by HF washing, the oxide layer thickness was determined to be 10 nm from the image.

Finite Element Model for Calculating Diffusion-Induced Stresses

We hypothesize that the outer wall can serve as a mechanical constraining layer to hold the external surface of the DWSiNTs static while forcing the Si expansion inwards into the hollow core. To understand the mechanical constraining effects of the outer oxide wall, we have conducted finite element simulations to model the stress evolution and deformation behavior during lithiation. In the model, the amorphous Si wall is the active material that reacts with the lithium ions. Lithium can also react with SiOx, although its reaction is not reversible and its products, such as lithium silicates and oxides, are mechanically strong materials. We assume that Li ions react with the SiOx layer before diffusing into the Si nanotubes, which will result in the formation of lithium silicate. For simplicity, we describe lithiation of the Si nanotubes only after the SiOx layer is fully lithiated. We also assume that the lithiated SiOx layer is sufficiently thin to be flaw-tolerant, so that fracture of the oxide would not occur during subsequent lithiation of the Si naotubes.

The core of the nanotube in an unlithiated state is given mechanical properties of amorphous Si (Young's modulus of 80 GPa, Poisson's ratio of 0.22, and yield strength of 1.0 GPa), and the 10nm thick surface oxide is given mechanical properties of lithiated phase of $Li_2Si_2O_5$ (Young's modulus of 90 GPa, Poisson's ratio of 0.17, yield stress of 2.52GPa which is evaluated from the hardness of 9GPa and approximated Tabor factor of 2.5 (Ref. 1)). The core of the Si naotube in a lithiated state is given the following mechanical properties (Young's modulus of 15 GPa, and yield strength of 60MPa). The yield strength of 60 MPa is used in light of recent preliminary nanoindentation experiments on lithiatated Si, which show that the yield strength of lithiated Si might be much lower than reported by Sethuraman et al (Ref. 2). The SiO_2 layer is modeled as elastically isotropic for simplicity. The diffusion of lithium ion is modeled by the analogy of heat transfer with diffusion. The diffusion coefficient is assumed to be a function of Li concentration in order to consider the pressure gradient effect on the flux. Constant Li ion flux charging conditions are used as a boundary condition imposed at the interface to prevent oxide shell from swelling. Complete and detailed modeling procedures are described in another paper (Ref. 3).

Fig. S5 and S6 show the hoop stress evolution during lithiation in Si nanotubes with and without the outer oxide constraining layer. In Si nanotubes without the oxide wall, the outer region is in compression and the inner region is in tension during lithiation (Fig. S5a and S6a). In this case, the main source of stress generation is the volumetric strain gradient. However, the addition of the coating layer causes a strong compressive stress due to the constraining effect from the outer lithium silicate layer.

Therefore, stresses mainly result from the amount of volumetric strain itself, not from its gradient (Fig. S5b and S6b). This different mechanism for stress generation is revealed by the fact that the maximum stress occurs at a very early stage in Si nanotubes, while DWSiNTs show maximum stress at 12.5% of the fully lithiated state (Fig. S6). As a result, the oxide-free Si nanotubes expand outward during lithiation, while the oxide wall of DWSiNTs forces the Si to only expand inward (supplementary movie S1, S2).

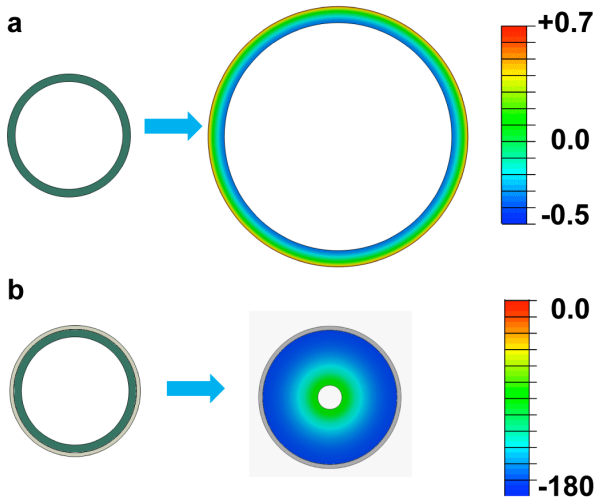

Figure S5. Theoretical modeling of hoop stress distribution before and after lithiation in single-walled Si nanotubes without surface coating (**a**) and DWSiNTs (**b**). Left column: Initial geometry of nanotubes. Right column: Hoop stress distribution through the wall of the nanotubes in the lithiated state. The unit of stress is MPa.

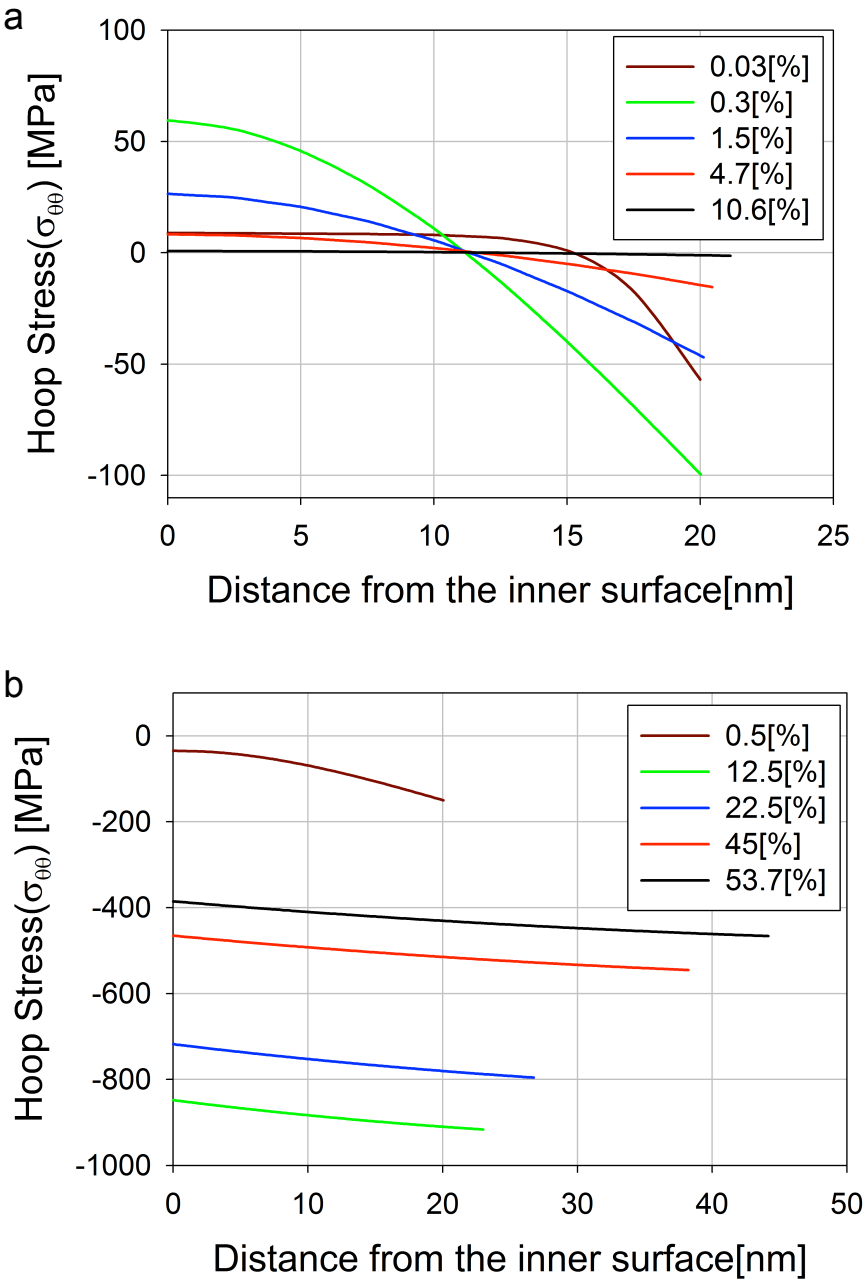

Figure S6. Theoretical modeling of stress distribution during lithiation in Si nanotubes. Hoop stresses through the wall of the single walled Si nanotubes (SWSiNT) (a) and DWSiNT (b) at different lithiation times are plot due to lithiation at a rate of 0.1 C. The dimension of the nanotubes is as follows: SWSiNT, R_{in}~140 nm, R_{out}~ 160 nm; DWSiNT, R_{in}~140 nm, R_{out}~ 160 nm, Thickness of oxide~10nm.

Ex-situ TEM battery cycling for a single Si nanotube

In order to observe the volume expansion of a single identical nanotube before and after full lithiation, battery cells were cycled using TEM grids as working electrode substrates (Fig. S7). For these processes, TEM grids with reference marks (Ted Pella) were used. Titanium layers (~20 nm) were deposited by e-beam evaporation onto original carbon films on the grids to ensure good electrical contacts between a Si nanotube and the grid surface. Si nanotubes were dissolved in methanol by sonication and then several drops of the solution were dropped onto the TEM grids to form TEM grid-based anodes. Before battery cell preparation, nanotubes were imaged by TEM and each nanotube's location relative to reference marks was recorded. For battery cycling, pouch cells were made. TEM grid-based anodes were located on copper current collectors and then separators (Asahi Kasei) soaked with electrolyte (1 M $LiPF_6$ in ethylene carbonate/diethyl carbonate (EC/DEC, 1:1 v/v, Ferro Corporation)) and Li foils (Alfa Aesar) were placed on top sequentially. After cycling, TEM grid-based anodes were rinsed with acetonitrile thoroughly and then delivered to TEM in sealed vials. TEM grids were loaded into the TEM chamber within 15 sec to minimize the period of the exposure to air. Finally, we found the original nanotubes using the reference marks on TEM grids.

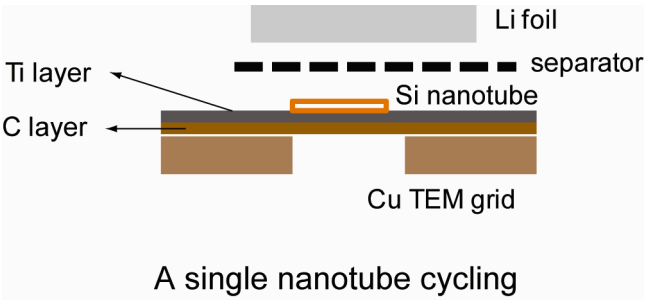

Figure S7. Schematic illustration of a TEM pouch cell used for the battery cycling with a single nanotube.

This mechanical constraining effect was confirmed experimentally by tracking a single nanotube before and after lithiation by TEM observation. As shown in supplementary Fig. S8, a DWSiNT with inner diameter (ID) of 209 ± 2 nm and outer diameter (OD) of 294 ± 2 nm before lithiation has ID of 156 ± 4 nm and OD of 293 ± 3 nm after full lithiation. Thus, only inward expansion in DWSiNTs was observed after full lithiation of silicon. We have confirmed this general observation through TEM experiments of more individual DWSiNTs (Supplementary Table S1). Note that the thickness of the electrode layer remains unchanged during the electrochemical reactions due to the steady outer surface of each single tube.

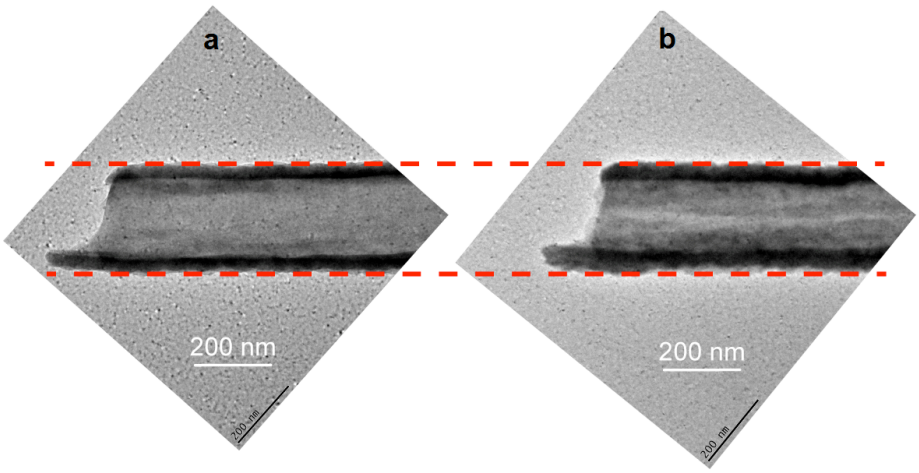

Figure S8. TEM images of an individual DWSiNT before (a) and after (b) lithiation, respectively. They show the tube wall expanded towards the inside, while the outside diameter of the tube remains constant.

	Outer Diameter (OD,nm)		Inner Diameter (ID,nm)		OD Increased (nm)	ID Decreased (nm)
	Before Lithiation	After Lithiation	Before Lithiation	After Lithiation		
DWSiNTs						
No.1	372	376	282	220	4	62
No.2	384	384	309	238	0	71
No.3	471	467	335	273	−4	62
No.4	419	420	336	277	1	59
No.5	442	438	347	255	−4	92
No.6	580	575	319	235	−5	84
No.7	294	293	209	156	−1	53
SWSiNTs						
No. 8	397	460	338	364	63	−26
No. 9	409	461	349	280	52	−29

Table S1. Ex-situ TEM observation of single nanotubes before and after lithiation. Inner diameter (ID) and outer diameter (OD) for SiO_2 clamped double walled silicon nanotube (DWSiNTs) and single walled Si nanotubes (SWSiNTs) without mechanical constraining were recorded in the table.

Expansion of SiO_x in DWSiNTs during lithiation

Both our experimental results and model analysis show that the expansion of SiO_x is small enough compared to that of Si and can be neglected here:

First, we observed no expansion of the outer diameter of the whole tube from experimental results. As shown in Figure S6 and Table S1, there is no change in the outer diameter of the Si/SiOx double walled tube after lithiation. If the outer layer of SiOx expanded significantly, we should have been able to measure the outer diameter increase. But this was not the case.

Second, our simulation indicates that the expansion due to SiOx layer is small (about 10-20% depending on the lithium concentration), comparable to graphite (~10%). The expansion of SiOx is one order magnitude smaller than that of Si (up to 400%). In the simulation, we used the same dimension as that in strain simulation (Figure S4, DWSiNT, R_{in}~140 nm, R_{out}~ 160 nm, Thickness of oxide~10nm), hence the radius of the double walled tube was 170 nm. We considered two sates of charging (1000 mAh/g and 3000 mAh/g for a-Si) with two compositions of the oxide layer (SiO_2 and SiO). In each case, we supposed that the boundary between oxide clamping layer and amorphous silicon remained intact, to determine how the expansion of the oxide layer affected the volume change of the whole tube.

The reaction of SiOx layer with Li^+ is taken to be (Ref 4):

$$SiO_x + (2x+y)\,Li \rightarrow Li_ySi + x\,Li_2O$$

We supposed a linear relation between volume expansion and state of charging between 0 and 4000 mAh/g (Si and $Li_{4.4}Si$, 300% expansion in volume), as supported

by previous studies (Ref 5). Thus, at a capacity of z mAh/g, the volume of Li_ySi is (1+3z/4000) %.

Material	Density used in simulation (unit: g/cm^3):
SiO_2	2.5
SiO	2.1
a-Si	2.1
Li_2O	2.0

Before expansion, the volume for SiOx with mass *m* is $V_0=m/\rho_{oxide}$

After charging, the volume for the oxide layer is

$$V = (m\frac{M_{a-Si}}{M_{SiOx}} / \rho_{a-Si}) p_{capacity} + m(1 - \frac{M_{a-Si}}{M_{SiOx}})\frac{M_{Li2O}}{M_O} / \rho_{Li2O},$$

where $P_{capacity}$ is the volume of lithiated oxides/volume of SiO_x (e.g. (1+ 3*3000/4000) =2.25 for 3000 mAh/g). *M* with subscript is the molecular weight of the subscript material.

The outer diameter of the tube *d* after lithiation satisfied:

$$(d^2\text{-}160^2) / (170^2\text{-}160^2) = V/V_0,$$

and the volume change of the whole double-walled tube is $d^2/d_0^2\text{-}1$

Based on this model, we found that the expansion due to expansion of the oxide layer is:

	1000 mAh/g	3000 mAh/g
SiO	9.4%	20.3%
SiO_2	14%	23%

It is well known that the volume expansion of graphite is ~10% when it is fully converted to LiC_6 phase (Ref 6). The volume change of the whole tube due to expansion of the oxide layer is comparable to graphite and much less than silicon itself (up to 400%). We believe that our simulation further proved the advantage of

double walled tube structure.

Electrolyte Wetting inside Si Nanotubes

Due to the tubes' continuous structure, the electrolyte does not wet the inside of the tubes even if there is a capillary force present, which can be confirmed by direct observation of a DWSiNT after immersing in electrolyte and drying (Fig. S9). Also, the lack of electrolyte wetting inside the tubes does not allow for SEI formation there. To demonstrate this, we have used a focused ion beam to slice open the DWSiNTs after cycling. Fig. S10 shows SEM images of cycled DWSiNTs after slicing; these images clearly show that there is no SEI formation inside the hollow space of DWSiNTs.

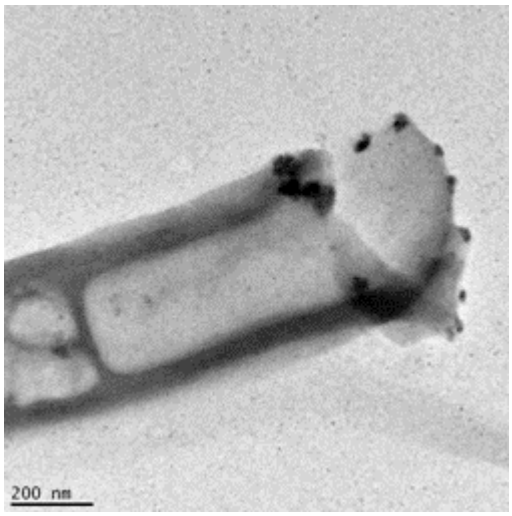

Figure S9. TEM image of a single tube after immerge into electrolyte and dried, showing the electrolyte wetted into nanotubes for only ~ 500 nm.

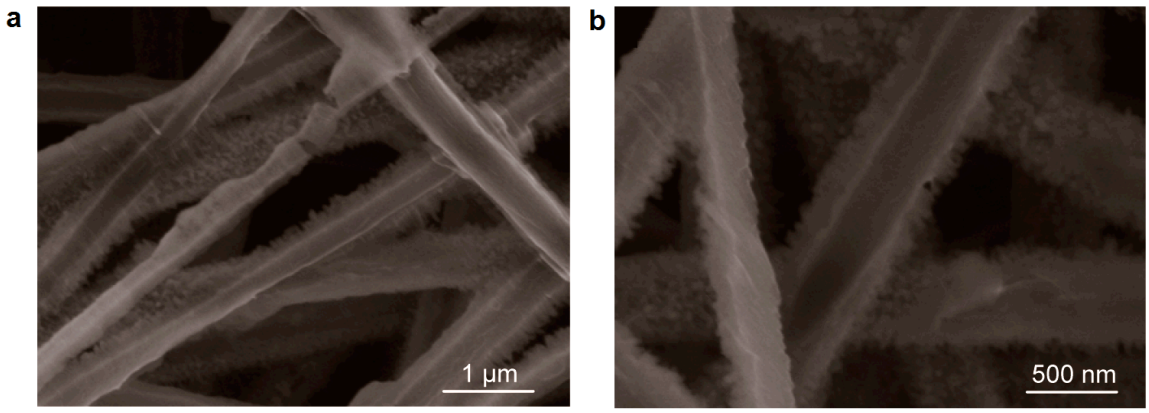

Figure S10. SEM images of DWSiNTs after cycling. The tubes have been cut by ion beams to expose inner structures. An argon ion beam at 1kV and 0.6μA was used here to slowly sputter etch the DWSiNFs for 2 minutes.

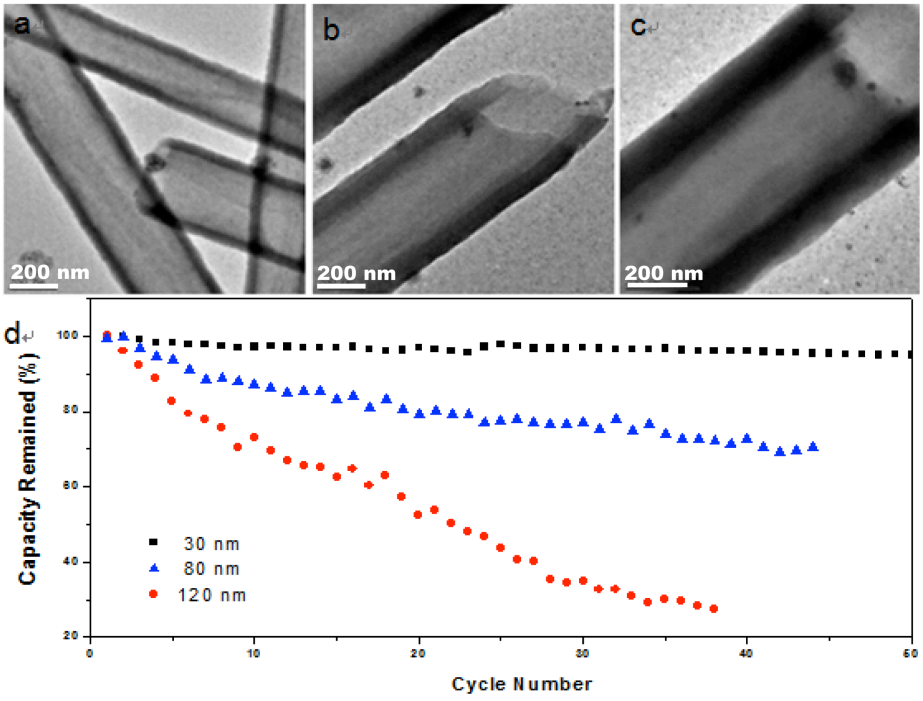

Figure S11. Electrochemical properties of DWSiNTs with different side wall thicknesses. (a-c) TEM images of DWSiNTs with wall thickness of (a)30 nm, (b) 80 nm, (c) 120 nm. The wall thicknesses were controlled by adjusting silicon deposition time. (d) capacity retention of DWSiNTs with different side wall thicknesses.

We note that our proposed working mechanisms are substantially different from previous single wall Si nanotube studies (Ref. 7-9), in which no static interface between silicon and the electrolyte have been designed since Si nanotube would expand towards outside. Our proposed structure is very different from the carbon-coated silicon nanotubes designed by Hertzberg et.al (Ref. 7) in which the Si material shrink and only has point contact with carbon wall. The detachment of Si from carbon creates capacity fading and present bottlenecks for lithium diffusion into Si since Li needs to diffuse through the point contact, resulting in poor rate performance. In our design here, Si remain as bonding to the constrain wall, and there is no lithium diffusion problem. In addition, we provide direct and clear evidences of stable SEI formation in our study, which are absent in Ref. 7. Moreover, in the carbon-Si nanotube structures of Ref. 7, there are no evidence that the inner Si surface is free of electrolyte wetting and thus the establishment of stable Si-electrolyte interphase can not be confirmed there.

Reference:

(1) Soares P. & Lepienski C.M., Residual stress determination on lithium disilicate glass-ceramic by nanoindentation. *J. Non-crystalline Solids* **348***,* 139-143 (2004)

(2) Sethuraman V. A., Chon M. J., Shimshak M., Srinivasan V. & Guduru P. R., In situ measurements of stress evolution in silicon thin films during electrochemical lithiation and delithiation. *J. Power Sources* **195,** *5062* (2010)

(3) Ryu I., Choi J. W., Cui Y. & Nix W.D., Size-dependent fracture of Si nanowire battery anodes *J. Mech. Phys. Solids*, **59,** 1717-1730 (2011)

(4) Sun Q.**,** Zhang B. & Fu Z., Lithium electrochemistry of SiO_2 thin film electrode

for lithium-ion batteries. *Appl. Surf. Sci.* **254***,* 3774-3779 (2008)

(5) He Y., Yu X., Li G., Wang R., Li H., Wang Y., Gao H. & Huang X., Study on the volume expansion of amorphous and microcrystalline silicon during lithium insertion and extraction. *LiBD-5– Electrode materials,* Arcachon, France (2011)

(6) Zou L.**,** Kang F.**,** Zheng Y. & Shen W., Modified natural flake graphite with high cycle performance as anode material in lithium ion batteries, *Electrochim. Acta* **54,** 3930-3934 (2009)

(7) Hertzberg, B., Alexeev, A. & Yushin, G. Deformations in Si-Li Anodes Upon Electrochemical Alloying in Nano-Confined Space. *J. Am. Chem. Soc.***132**, 8548-8549 (2010).

(8) Song, T. *et al.* Arrays of Sealed Silicon Nanotubes As Anodes for Lithium Ion Batteries. *Nano Lett.* **10**, 1710-1716 (2010).

(9) Park, M. H. *et al.* Silicon Nanotube Battery Anodes. *Nano Lett.* **9**, 3844-3847 (2009).

Supporting Movie Captions:

Movie 1. Hoop stress distribution during lithiation in SWSiNT at different lithiation times due to lithiation at a rate of 0.1 C. The initial dimension of the Si naotube is as follows (R_{in}~140 nm, R_{out}~ 160 nm). The unit of stress showing in the movie is TPa.

Movie 2. Hoop stress distribution during lithiation in DWSiNTs at different lithiation times due to lithiation at a rate of 0.1 C. The initial dimension of the naotubes is as follows (R_{in}~140 nm, R_{out}~ 160 nm, Thickness of oxide~10nm). The unit of stress showing in the movie is TPa.